Received December 3, 2019, accepted December 11, 2019, date of publication December 19, 2019, date of current version December 31, 2019.

Digital Object Identifier 10.1109/ACCESS.2019.2960864

Optimal Control of Ascent Trajectory for Launch Vehicles: A Convex Approach

YUAN LI[1], YINGZI GUAN[1], CHANGZHU WEI[1], AND RENYI HU[2]
[1]Harbin Institute of Technology, Harbin 150001, China
[2]Beijing Aerospace Automatic Control Institute, Beijing 100000, China

Corresponding author: Changzhu Wei (weichangzhu@hit.edu.cn)

This work was supported in part by the National Natural Science Foundation of China under Grant 61403100, and in part by the Foundational Innovation Team Support Program under Grant 2017cx023.

ABSTRACT This paper presents an online ascent trajectory optimization algorithm based on optimal control and convex optimization without accurate initial guesses. Due to the high complexity of space systems, exceptional cases such as engine failures may happen during the flight. In these cases, the dynamical model greatly changes and the nominal trajectory is infeasible. Thus, online trajectory optimization and replan should be considered when accurate initial guesses cannot be given. In this paper, the ascent trajectory optimization problem of launch vehicles is formulated as a Hamilton two-point boundary value problem (TPBVP) according to the optimal control theory. The control vector is expressed as a function of costate variables and the terminal condition is given according to the orbital constraint of the launch mission. In order to solve the TPBVP rapidly and accurately without accurate initial guesses, a convex approach is presented. Firstly, the flip-Radau pseudospectral method is applied to convert the continuous-time TPBVP into a finite-dimensional equality constraint. Then, successive linearization is applied to formulate the problem as a series of iteratively solved second-order cone programming (SOCP) subproblems. Considering the accuracy and robustness of the algorithm, trust-region and relaxation strategy are applied. The convex trajectory optimization can be solved by Interior Point Method (IPM) automatically. Simulation results in the case of thrust loss are presented to show the accuracy, efficiency and robustness of the algorithm.

INDEX TERMS Launch vehicle, optimal control, convex optimization, initial guess, terminal constraints.

I. INTRODUCTION

With the development of space engineering, the requirements of reliability and intelligence of the vehicles under different launch missions is becoming increasingly higher. However, the increasing complexity of the space system causes a higher probability of emergencies, such as Proton-M in 2014, LM-V in 2017. In these cases, the dynamical model changes greatly and the nominal trajectory becomes infeasible. Therefore, the trajectory needs to be replanned automatically according to the orbital mission, which is called onboard trajectory planning [1]. Without ground support, the onboard trajectory planning should be both accurate and rapid. Considering the unpredictability of the emergency during the flight, the robustness of the algorithm when the initial guess is inaccurate needs to be improved. In this paper, a convex approach to solve the optimal control problem of ascent trajectory is presented for online trajectory planning. The proposed technology can also be applied to the missions of space station, manned moon landing and deep-space exploration to improve reliability.

The associate editor coordinating the review of this manuscript and approving it for publication was Md Asaduzzaman.

In general, the ascent trajectory planning problem of launch vehicles [2]–[4] and ground vehicles [5] can be formulated as an optimal control problem. Based on the dynamical model, the velocity and position of the vehicle are presented as functions of the thrust vector, which is always defined as the optimal variable. The objective of the optimization for this problem can be maximum-energy, minimum-time or minimum-fuel-consumption. Other constraints including the initial condition, path constraint, and terminal orbital constraint also need to be considered as part of the optimal control problem, multiobjective constrained trajectory optimization problem is studied in [6]. The optimal control of ascent trajectory with complex constraints and high nonlinear dynamics is a great challenge for onboard optimization. In general, the indirect [7]–[10] and direct [11] methods are mainly applied to solving the optimal control problems. As for the indirect method, the optimal control problem is converted into Hamilton two-point boundary value problems (TPBVP) based on the Minimum Principle. Because of the optimal condition with multiple constraints, the TPBVP is always very complex and highly sensitive to the initial guess. Therefore, the convergence and robustness of the optimization algorithm based on the indirect method is always unsatisfactory. Stochastic method has been applied to solve the TPBVP under uncertain conditions [12], [13], but for the extreme conditions such as engine failure, the study is very few. Another widely applied method for trajectory optimization is the direct method, which transforms the trajectory optimization into a nonlinear programming problem (NLP) [11] and solves it by NLP algorithms. However, the computational time of general NLP algorithms is too long, which cannot meet the onboard real-time requirement. And it is well known that the NLP algorithms are easily trapped in local optimum.

In recent years, convex optimization techniques have been widely studied [14], [15]. As a subclass of convex optimization, second-order cone programming (SOCP) problems can be solved in polynomial time with no need for initial guesses supplied by users based on the interior-point method (IPM) [15], which is very appealing to onboard optimization applications. However, most optimization problems in practice do not have the specific form required in SOCP. That is, the objective function should be linear, subject to linear equality constraints and second-order cone inequality constraints [15]. Most researchers focus on transforming nonconvex optimal problems into problems within the convex framework, which is called convexification. Several techniques have been successfully applied such as lossless convexification [16]–[19] and successive convexification. However, due to the accuracy and trust-region constraint of the successive convexification, the global optimization of the solution cannot be guaranteed. The convex optimization techniques have been successfully applied in powered landing vehicles [20], rockets [21]–[22],UAVs [23], spacecrafts [24], high-speed atmospheric vehicles [25], etc. [26], [27].

In order to solve the optimal control problem of ascent trajectory, especially under emergencies without accurate initial guesses, this paper presents a convex approach to solve the TPBVP transformed from the original trajectory optimization problem. Based on the dynamical model and optimal control theory, the differential equations of state and costate variables are given. To guarantee the optimality of the solution, the optimality condition is also considered in the differential equations. As for terminal constraints, five orbital elements are considered except the true anomaly, and the equality constraints are expressed in the perifocal coordinate system for convenience. Then, the optimal control problem of ascent trajectory is transformed into a free-final-time TPBVP, which is highly nonlinear. In order to solve the TPBVP accurately and efficiently, especially under emergencies without accurate initial guesses, a convex approach is proposed. Firstly, the TPBVP is discretized by the flip-Radau pseudospectral method and converted into a series of equality constraints. Then, successive convexification is used to handle the nonconvexity. In addition, the trust-region and relaxation strategy are employed to improve the accuracy and robustness of the algorithm. The algorithm proposed in this paper can be applied to the online ascent trajectory replanning in case of emergencies without accurate initial guesses.

This paper is organized as follows. In Section II, the optimal control problem of the ascent trajectory is described in detail, and the TPBVP is given. In Section III, the continuous-time TPBVP is transformed into a series of iteratively solved finite-dimensional convex optimization subproblems by diecretization and successive convexification techniques. In section IV, simulations are carried out to demonstrate the robustness, efficiency and accuracy of the presented algorithm. In Section V, conclusions are drawn.

II. OPTIMAL CONTROL PROBLEM FORMULATION

In this section, a brief description about the dynamical model of launch vehicles is presented as the preliminary. Then, the optimal control problem of ascent trajectory is formulated in detail. Finally, the TPBVP of ascent trajectory optimization is given.

A. DYNAMICAL MODEL

In this paper, we formulate the equations of motion of launch vehicles in the Earth Center Inertial Coordinate System [28]. The dimensionless equations can be expressed as follows:

$$\begin{aligned} \dot{\boldsymbol{r}} &= \boldsymbol{V} \\ \dot{\boldsymbol{V}} &= -\frac{1}{\|\boldsymbol{r}\|^3}\boldsymbol{r} + \frac{T}{mg_0}\boldsymbol{I}_b \\ \dot{m} &= -\frac{T}{g_0 I_{sp}} \cdot \sqrt{\frac{R_0}{g_0}} \end{aligned} \tag{1}$$

where $\boldsymbol{r}$ and $\boldsymbol{V} \in R^3$ are the dimensionless inertial position and velocity vectors, respectively; m is the mass of the launch vehicle. g_0 represents the gravitational acceleration magnitude on the surface of the Earth. I_{sp} represents the specific impulse of the engine. The distance is normalized by R_0(the radius of the Earth at equator), the time by $\sqrt{R_0/g_0}$, and the velocity by $\sqrt{R_0 g_0}$ [28]. As the thrust magnitude of the rocket engine T is constant, $\boldsymbol{I}_b$ is the unit vector of body axes satisfying:

$$\|\boldsymbol{I}_b\| \equiv 1 \tag{2}$$

The trajectory optimization problem of launch vehicles is defined as an optimal control problem to achieve the minimum fuel consumption. As the mass flow is constant, the optimal ascent problem can be treated as a minimum-time problem:

$$\min J = t_f \tag{3}$$

where t_f is the flight time.

B. HAMILTONIAN FUNCTION

In this paper, the mass of the vehicle is treated as a prescribed function of time instead of a state variable. Based on the optimal control theory, the Hamiltonian function is defined as:

$$H = \boldsymbol{p}_r^T \boldsymbol{V} + \boldsymbol{p}_V^T \left(-\frac{\boldsymbol{r}}{\|\boldsymbol{r}\|^3} + \frac{T}{mg_0} \boldsymbol{I}_b \right) + \mu \left(\boldsymbol{I}_b^T \boldsymbol{I}_b - 1 \right) \tag{4}$$

where $\boldsymbol{p}_r$ and $\boldsymbol{p}_V \in R_3$ are the costate vectors, and μ is a scalar constraint multiplier.

According to the first order necessary conditions for the optimal control problem, the differential equations of the costate variables are:

$$\begin{aligned} \dot{\boldsymbol{p}}_r &= -\frac{\partial H}{\partial \boldsymbol{r}} = \frac{1}{\|\boldsymbol{r}\|^3} \boldsymbol{p}_V - \frac{3 \boldsymbol{p}_V^T \boldsymbol{r}}{\|\boldsymbol{r}\|^5} \boldsymbol{r} \\ \dot{\boldsymbol{p}}_V &= -\frac{\partial H}{\partial \boldsymbol{V}} = -\boldsymbol{p}_r \end{aligned} \tag{5}$$

C. OPTIMALITY CONDITION

Considering the maximum principle of the Hamiltonian function, the optimality condition is:

$$H \left(\boldsymbol{p}_r, \boldsymbol{p}_V, \boldsymbol{r}^*, \boldsymbol{V}^*, \boldsymbol{I}_b^*, t \right) = \max_{\boldsymbol{I}_b} H \left(\boldsymbol{p}_r, \boldsymbol{p}_V, \boldsymbol{r}^*, \boldsymbol{V}^*, \boldsymbol{I}_b, t \right) \tag{6}$$

where the superscript "$*$" represents the solution of the optimal control problem. The optimality condition can also be expressed as:

$$\frac{\partial H}{\partial \boldsymbol{I}_b} = 0 \tag{7}$$

Based on (4), we have

$$\frac{\partial H}{\partial \boldsymbol{I}_b} = \frac{T}{mg_0} \boldsymbol{p}_V + 2\mu \boldsymbol{I}_b = 0 \tag{8}$$

which yields

$$\boldsymbol{I}_b = -\frac{T}{2\mu mg_0} \boldsymbol{p}_V \tag{9}$$

According to the optimal control theory [28], the optimal body axes (thrust vector) direction should be along the direction of $\boldsymbol{p}_V$, which is

$$\boldsymbol{I}_b = \frac{\boldsymbol{p}_V}{\|\boldsymbol{p}_V\|} \tag{10}$$

D. TERMINAL CONDITIONS

As for the optimal control problem of ascent trajectory, the terminal conditions include orbital insertion conditions and transversality conditions. For most launch missions, the orbital insertion conditions include orbital elements which depend on the final position and velocity. Orbital elements include the semi-major axis, eccentricity, inclination, longitude of the ascending node, argument perigee and true anomaly $[a, e, i, \Omega, \omega, f]$ [29]. Except for some fixed injection point tasks, the true anomaly is always ignored.

In this paper, the terminal constraints are expressed in the perifocal coordinate system for convenience. Considering the accuracy of the orbital plane, the following constraints must be ensured:

$$\begin{aligned} [0, 0, 1]^T \boldsymbol{r}_f &= 0 \\ [0, 0, 1]^T \boldsymbol{V}_f &= 0 \end{aligned} \tag{11}$$

where the subscript "f" represents the final value, $\boldsymbol{r}_f$ and $\boldsymbol{V}_f$ are the final position and velocity vector in the perifocal coordinate system.

For orbital launch missions, the final position must be on the target orbit. According to the ellipse equation, the final position vector $\boldsymbol{r}_f$ must satisfy:

$$\frac{\left(r_{fx} + c \right)^2}{a^2} + \frac{r_{fy}^2}{b^2} - 1 = 0 \tag{12}$$

where b is the semi-minor axis and $b = a^2 \left(1 - e^2 \right)$, c is the distance from the center of earth to the center of ellipse orbit and $c = ae$.

Differentiating (12) yields:

$$\frac{\left(r_{fx} + c \right) V_{fx}}{a^2} + \frac{r_{fy} V_{fy}}{a^2 \left(1 - e^2 \right)} = 0 \tag{13}$$

This equation is also the constraint of the direction of the final velocity.

Finally, considering the conservation of angular momentum, we obtain:

$$r_{fx} V_{fy} - r_{fy} V_{fx} - h = 0 \tag{14}$$

where $h = \sqrt{a \left(1 - e^2 \right)}$ is the required magnitude of angular momentum.

As for a circular target orbit, the terminal constraints (12)~(14) can be replaced by the following equations:

$$\begin{aligned} r_{fx}^2 + r_{fy}^2 - a^2 &= 0 \\ r_{fx} V_{fx} + r_{fy} V_{fy} &= 0 \\ V_{fx}^2 + V_{fy}^2 - \sqrt{1/a} &= 0 \end{aligned} \tag{15}$$

The orbital insertion conditions for entering the target orbit of space vehicles are (11)~(14) or (11)&(15). In this paper, those conditions are expressed as:

$$\boldsymbol{\psi} \left(\boldsymbol{r}_f, \boldsymbol{V}_f \right) = 0 \tag{16}$$

Besides the orbital insertion conditions, the following transversality conditions must also be satisfied:

$$\boldsymbol{p}_f = \frac{\partial \phi}{\partial \boldsymbol{x}_f} + \boldsymbol{\xi}^T \frac{\partial \boldsymbol{\psi}}{\partial \boldsymbol{x}_f} \tag{17}$$

$$H \left(\boldsymbol{p}_r, \boldsymbol{p}_V, \boldsymbol{r}^*, \boldsymbol{V}^*, \boldsymbol{I}_b^*, t \right) \big|_{t_f} = \frac{\partial \phi}{\partial t_f} \tag{18}$$

where $\boldsymbol{\xi}$ is a constant multiplier vector. $\boldsymbol{p}_f = \left[\boldsymbol{p}_{rf}, \boldsymbol{p}_{Vf} \right]$ and $\boldsymbol{x}_f = \left[\boldsymbol{r}_f, \boldsymbol{V}_f \right]$. $\frac{\partial \boldsymbol{\psi}}{\partial \boldsymbol{x}_f}$ is shown in appendix. (17) can be formulated as a equality constraint of $\boldsymbol{p}_f$ and $\boldsymbol{x}_f$. ϕ is the performance index.

E. TWO-POINT-BOUNDARY-VALUE PROBLEM

In conclusion, the optimal control problem of ascent trajectory is transformed into a free-final-time two-point-boundary-value problem (TP 1) including differential equations of state and costate variables, optimality conditions, initial and terminal conditions:

TP 1:

$$\begin{aligned} \dot{\boldsymbol{r}} &= \boldsymbol{V} \\ \dot{\boldsymbol{V}} &= -\frac{1}{\|\boldsymbol{r}\|^3}\boldsymbol{r} + \frac{T}{mg_0}\frac{\boldsymbol{p}_V}{\|\boldsymbol{p}_V\|} \\ \dot{m} &= -\frac{T}{g_0 I_{sp}} \cdot \sqrt{\frac{R_0}{g_0}} \end{aligned} \tag{19}$$

$$\begin{aligned} \dot{\boldsymbol{p}}_r &= \frac{1}{\|\boldsymbol{r}\|^3}\boldsymbol{p}_V - \frac{3\boldsymbol{p}_V^T\boldsymbol{r}}{\|\boldsymbol{r}\|^5}\boldsymbol{r} \\ \dot{\boldsymbol{p}}_V &= -\boldsymbol{p}_r \end{aligned} \tag{20}$$

$$\boldsymbol{x}(t_0) = \boldsymbol{x}_0 \tag{21}$$

$$\bar{\boldsymbol{\psi}}\left[\boldsymbol{x}\left(t_f\right), \boldsymbol{p}\left(t_f\right)\right] = 0 \tag{22}$$

where the variable $\boldsymbol{x} = [\boldsymbol{r}, \boldsymbol{V}]$. (21) is the inertial constraints and (22) is the terminal conditions. $\bar{\boldsymbol{\psi}}$ includes orbital insertion conditions $\boldsymbol{\psi}$ and transversality conditions (17)&(18).

III. CONVEXIFICATION ALGORITHM

In this section, in order to solve TP 1 reliably and efficiently, a convex approach is adopted. Firstly, the flipped-Radau pseudospectral method is employed to discretize the problem into a finite-dimensional problem. Then the discretized problem is transformed into a series of convex subproblems. Those subproblems can be solved by IPM and the solution will be convergent during the iteration.

A. PSEUDOSPECTRAL DISCRETIZATION

In Section II, the optimal control problem of ascent trajectory is transformed into a TPBVP. However, because of the differential equations of state and costate variables, the optimization problem is an infinite-dimensional one that is difficult to be solved by numerical methods. Discretization is a commonly used method to transform the continuous-time optimal control problem into a series of finite-dimensional problems. The detailed discussion about discretization methods and the selection of optimal variables can be found in [30]. In this paper, considering both efficiency and accuracy of the algorithm, the flip-Radau pseudospectral method is applied to convert (19) and (20) into a series of zero finding problems. The discretization equation of the state and costate variables is:

$$\sum_{j=0}^{N} \boldsymbol{D}_{ij}\bar{\boldsymbol{x}}\left(\tau_j\right) - \frac{t_f}{2}\boldsymbol{f}\left[\bar{\boldsymbol{x}}\left(\tau_j\right)\right] = 0, \quad (i = 1, \ldots, N) \tag{23}$$

where $\boldsymbol{D}$ is the flip-Radau pseudospectral differentiation matrix [31]; t_f is the flight time; $\boldsymbol{f}$ is the right-hand side of the differential dynamic equations (19) and (20), τ is the collocation points in the domain $(-1, 1]$. N is the number of the collocation points. $\bar{\boldsymbol{x}}$ is state and costate variables including $\boldsymbol{r}$, $\boldsymbol{V}$, m, $\boldsymbol{p}_r$ and $\boldsymbol{p}_V$

Considering that τ is defined in the domain (-1,1], the time domain $\left[t_0, t_f\right]$ is mapped into $[-1, 1]$ in the discretization as

$$\tau = \frac{2 \cdot t - t_f - t_0}{t_f - t_0}, \quad t \in \left[t_0, t_f\right] \tag{24}$$

TABLE 1. Parameters of the mission.

Initial Condition	V_{x0}, m/s	-3646.3
	V_{y0}, m/s	-3106.2
	V_{z0}, m/s	2147.2
	X_0, m	1.76e+06
	Y_0, m	4.34e+06
	Z_0, m	4.77e+06
Orbital Injection	Semi-major axis, m	7.72e+06
	Eccentricity	0.1288
	Inclination, deg	52.77
	Longitude of ascending node, deg	61.42
	Argument perigee, deg	71.01
	True anomaly, deg	4.96

TABLE 2. Deviations of terminal orbital elements.

Parameters	Deviations
Semi-major axis, m	3.28
Eccentricity	-0.00002
Inclination, deg	0.0003
Longitude of ascending node, deg	0.0001
Argument perigee, deg	-0.0002
True anomaly, deg	2.38

B. IMPROVED SUCCESSIVE CONVEXIFICATION

Now, the optimal control problem of ascent trajectory is transformed into a series of zero finding problems (22) and (23). In general, Newton method is adopted to solved these equations. However, Newton method requires accurate initial guesses for both state and costate variables. In general, the costate variable do not have any physical meaning, but the ascent trajectory is highly sensitive to the costate variable. This difficulty leads to algorithm divergence during the iteration by Newton method when the physical trajectory is greatly different from the nominal one. In this paper, convex optimization is employed to solve the zero finding problems without accuracy initial guesses.

The zero finding problems (22) and (23) are treated as nonlinear (nonconvex) equality constraints by convex optimization. In order to handle the nonconvexity, the first–order Taylor series expansion is used to approximate nonlinear

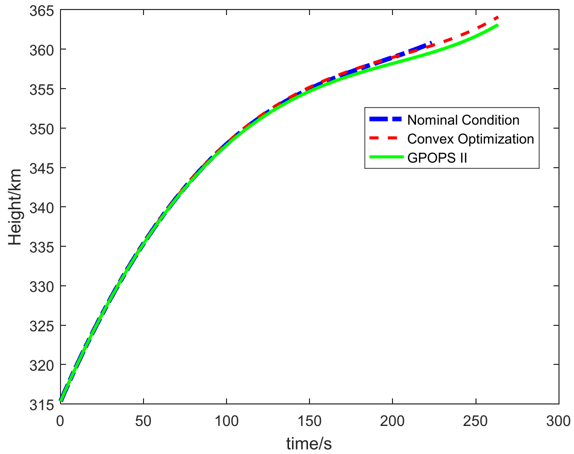

FIGURE 1. Curve of height.

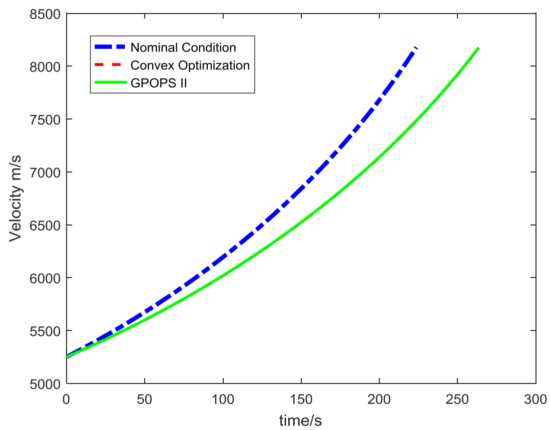

FIGURE 2. Curve of velocity.

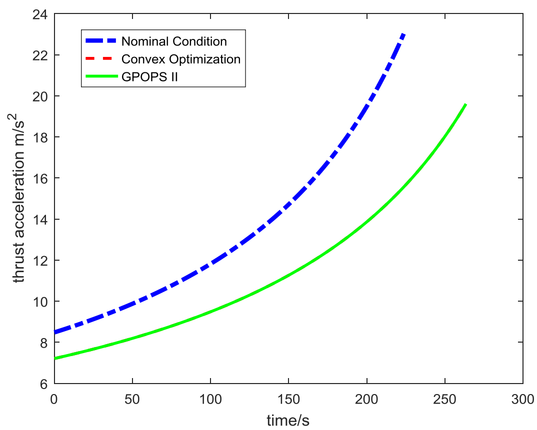

FIGURE 3. Curve of thrust acceleration.

functions (22) and (23):

$$2\boldsymbol{D}\left(\bar{\boldsymbol{x}}^k + \Delta\bar{\boldsymbol{x}}\right) - t_f\left[\boldsymbol{f}\left(\bar{\boldsymbol{x}}^k\right) + \frac{\partial \boldsymbol{f}\left(\bar{\boldsymbol{x}}^k\right)}{\partial \bar{\boldsymbol{x}}}\Delta\bar{\boldsymbol{x}}\right] - \boldsymbol{f}\left(\boldsymbol{x}_1^k, \boldsymbol{u}_1^k\right)\Delta t_f = 0 \tag{25}$$

$$\bar{\boldsymbol{\psi}}\left(\bar{\boldsymbol{x}}_f\right) + \frac{\partial \bar{\boldsymbol{\psi}}\left(\bar{\boldsymbol{x}}_f\right)}{\partial \bar{\boldsymbol{x}}_f}\Delta\bar{\boldsymbol{x}}_f = 0 \tag{26}$$

$$\begin{aligned} \bar{\boldsymbol{x}}^{k+1} &= \bar{\boldsymbol{x}}^k + \Delta\bar{\boldsymbol{x}} \\ t_f^{k+1} &= t_f^k + \Delta t_f \end{aligned} \tag{27}$$

where $\Delta\bar{\boldsymbol{x}}$ and Δt_f are the optimal variables. Considering the accuracy of linearization, the "trust-region" constraint is introduced:

$$\begin{aligned} \Delta\bar{\boldsymbol{x}} &\leq \boldsymbol{\varepsilon}_x \\ \Delta t_f &\leq \varepsilon_t \end{aligned} \tag{28}$$

At the beginning of the iteration, the initial solution always cannot satisfy the constraints (25) and (26) strictly considering the accuracy of linearization and initial guesses, even if the solution of the optimal control problem exists in fact, which is called "artificial infeasibility" [35]. In this case, there is no feasible solution of (25), (26) and (28), and the iteration cannot continue.

In order to avoid artificial infeasibility, the relaxation variables $\boldsymbol{\delta}_x$ and $\boldsymbol{\delta}_\psi$ are introduced, (25) and (26) are relaxed as [32]:

$$2\boldsymbol{D}\left(\bar{\boldsymbol{x}}^k + \Delta\bar{\boldsymbol{x}}\right) - t_f\left[\boldsymbol{f}\left(\bar{\boldsymbol{x}}^k\right) + \frac{\partial \boldsymbol{f}\left(\bar{\boldsymbol{x}}^k\right)}{\partial \bar{\boldsymbol{x}}}\Delta\bar{\boldsymbol{x}}\right] - \boldsymbol{f}\left(\boldsymbol{x}_1^k, \boldsymbol{u}_1^k\right)\Delta t_f = \boldsymbol{\delta}_x \tag{29}$$

$$\bar{\boldsymbol{\psi}}\left(\bar{\boldsymbol{x}}_f\right) + \frac{\partial \bar{\boldsymbol{\psi}}\left(\bar{\boldsymbol{x}}_f\right)}{\partial \bar{\boldsymbol{x}}_f}\Delta\bar{\boldsymbol{x}}_f = \boldsymbol{\delta}_\psi \tag{30}$$

where $\frac{\partial \boldsymbol{f}(\bar{\boldsymbol{x}})}{\partial \bar{\boldsymbol{x}}}$ is the linearized matrix, which is shown in Appendix. $\frac{\partial \bar{\boldsymbol{\psi}}(\bar{\boldsymbol{x}}_f)}{\partial \bar{\boldsymbol{x}}_f}$ can be calculated by numerical methods.

The magnitudes of $\boldsymbol{\delta}_\psi$ and $\boldsymbol{\delta}_x$ are considered in the objective function:

$$\min J = \left\|\boldsymbol{\delta}_\psi\right\| + \left\|\boldsymbol{\delta}_x\right\| \tag{31}$$

Specific implementation steps are as follows:

1) Set $k = 0$, and select initial state and costate variables $\bar{\boldsymbol{x}}^0$, $\boldsymbol{p}_0^0$ and t_f^0 based on the nominal trajectory. Give the trust region parameters $\boldsymbol{\varepsilon}_x$, ε_t and the accuracy requirement parameters ε, ε_δ.

2) Solve the convex subproblems (29), (30) and (31) by IPM, and calculate the update amount of the optimal variables.

3) Check the convergence condition:

$$\begin{aligned} \left\|\Delta\bar{\boldsymbol{x}}\right\| &< \varepsilon, \\ \left\|\boldsymbol{\delta}_\psi\right\| + \left\|\boldsymbol{\delta}_x\right\| &< \varepsilon_\delta \end{aligned} \tag{32}$$

If the convergence condition is satisfied, go to step 4, otherwise, set $k = k + 1$ and return to step 2.

4)The optimization problem is solved. The optimal variables are found to be $\bar{\boldsymbol{x}}^* = \bar{\boldsymbol{x}}^k$, $t_f^* = t_f^k$.

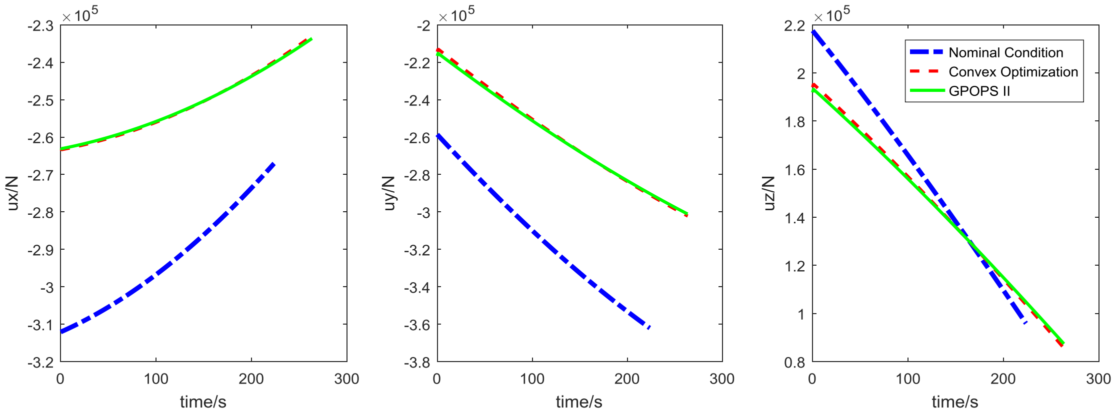

FIGURE 4. Curve of thrust vector.

IV. SIMULATIONS AND RESULTS

In this section, simulation verification is carried out by taking the last stage of the flight phase for a launch vehicle as the research object. In case of thrust loss, the numerical results are obtained to demonstrate the effectiveness and robustness of the proposed algorithm. In this case, the trajectory will be greatly different from the nominal one, without accurate initial guesses, traditional numerical methods based on Newton method cannot solve the TPBVP. In this paper, based on convex optimization, the optimal control problem is solved by the CVX [33] solver of MATLAB. For comparison, the solution obtained by GPOPS-II is given [34]. All numerical simulations in this paper are performed on a laptop with Intel Core i7 CPU 2.80GHz, and the MATLAB version is 2017a.

Parameters of the launch vehicle are as follows. The initial mass in the last stage is 54328kg; the thrust magnitude is 460kN; the effective exhaust velocity is 3000m/s. Parameters of the mission in the numerical experiment are listed in Table1 and Table2. The variables contained in this section's figures and tables are with respect to the Earth Centered Inertial coordinate system.

We assume that the thrust magnitude decreases by 15% and the rate of mass flow also decreases by 15% at the beginning of the flight, which means the effective exhaust velocity does not change. In this experiment, the number of collocation points is $N = 50$, the trust region parameters $\boldsymbol{\varepsilon}_x = 0.05$, $\varepsilon_t = 0.02$, and required accuracy parameters $\varepsilon = 10^{-5}, \varepsilon_\delta = 10^{-6}$. In addition, the initial guess of state variables $\boldsymbol{r}^0$ and $\boldsymbol{V}^0$ is given based on the nominal trajectory, and the initial guesses of costate variables are $\boldsymbol{p}_r^0 = 0, \boldsymbol{p}_V^0 = \boldsymbol{V}^0 / \|\boldsymbol{V}^0\|$.

As shown in Figure 1 ~ Figure 4 and Table 2, because of the thrust loss, the trajectory obtained by the algorithm is greatly different from the nominal trajectory, but the vehicle still can settle into the nominal target orbit accurately. And the solution of the present algorithm is identical to that of the traditional optimization method. Similar simulation results can be obtained based on different launch vehicles and launch missions in case of thrust loss, which demonstrates the accuracy and robustness of the algorithm proposed in this paper.

By the initial guess based on the nominal trajectory, the presented algorithm converges within seven iterations. In each iteration, it takes about 0.3 ~ 0.5 seconds to solve the convex optimization problem. It takes a CPU time of 77.98 seconds to achieve convergence by traditional method, and 3.21 seconds by proposed algorithm, which is only 4.1% of GPOPS-II's. Simulation results indicate satisfactory convergence of the presented algorithm, and this algorithm has great potential for onboard vehicle applications.

V. CONCLUSION

This paper presents an online ascent trajectory optimization algorithm for launch vehicles based on optimal control and convex optimization. Firstly, the optimal control problem of ascent trajectory based on the nondimensional dynamical model is formulated in detail. In order to solve the optimal control problem efficiently without accuracy initial guesses, a convex approach is proposed. Discretization, successive convexification and relaxation strategy are applied to improve the computational performance. In particular, this algorithm proves to enjoy strong robustness when the condition is greatly different from the nominal one without good initial guesses. Thus, this algorithm has potential applications in onboard trajectory optimization and re-planning for launch vehicles with no accurate initial guess under emergencies. In our follow-up work, we will extend the proposed algorithm by exploring the uncertainty during the flight of launch vehicles.

APPENDIX

The partial derivative of terminal constraint $\frac{\partial \boldsymbol{\psi}}{\partial \boldsymbol{x}_f}$ is:

1.For an elliptical target orbit

$$\frac{\partial \boldsymbol{\psi}}{\partial \boldsymbol{x}_f} = \begin{bmatrix} \frac{\partial \psi}{\partial \boldsymbol{r}} & \frac{\partial \psi}{\partial \boldsymbol{V}} \end{bmatrix} = \begin{bmatrix} 0 & 0 & 1 & 0 & 0 & 0 \\ 0 & 0 & 0 & 0 & 0 & 1 \\ \frac{2\left(r_{fx}+c\right)}{a^2} & \frac{2r_{fy}}{b^2} & 0 & 0 & 0 & 0 \\ \frac{V_{fx}}{a^2} & \frac{V_{fy}}{b^2} & 0 & \frac{r_{fx}+c}{a^2} & \frac{r_{fy}}{b^2} & 0 \\ V_{fy} & -V_{fx} & 0 & -r_{fy} & r_{fx} & 0 \end{bmatrix}$$

2.For a circular target orbit

$$\frac{\partial \boldsymbol{\psi}}{\partial \boldsymbol{x}_f} = \begin{bmatrix} \frac{\partial \psi}{\partial \boldsymbol{r}} & \frac{\partial \psi}{\partial \boldsymbol{V}} \end{bmatrix} = \begin{bmatrix} 0 & 0 & 1 & 0 & 0 & 0 \\ 0 & 0 & 0 & 0 & 0 & 1 \\ 2r_{fx} & 2r_{fy} & 0 & 0 & 0 & 0 \\ V_{fx} & V_{fy} & 0 & r_{fx} & r_{fy} & 0 \\ 0 & 0 & 0 & 2V_{fx} & 2V_{fy} & 0 \end{bmatrix}$$

The linearized matrix $\frac{\partial \boldsymbol{f}(\bar{\boldsymbol{x}})}{\partial \bar{\boldsymbol{x}}}$ is:

$$\frac{\partial \boldsymbol{f}(\bar{\boldsymbol{x}})}{\partial \bar{\boldsymbol{x}}} = \begin{bmatrix} \frac{\partial \dot{\boldsymbol{r}}}{\partial \bar{\boldsymbol{x}}} & \frac{\partial \dot{\boldsymbol{V}}}{\partial \bar{\boldsymbol{x}}} & \frac{\partial \dot{m}}{\partial \bar{\boldsymbol{x}}} & \frac{\partial \dot{\boldsymbol{p}}_r}{\partial \bar{\boldsymbol{x}}} & \frac{\partial \dot{\boldsymbol{p}}_V}{\partial \bar{\boldsymbol{x}}} \end{bmatrix}^T$$

$$\frac{\partial \dot{\boldsymbol{r}}}{\partial \bar{\boldsymbol{x}}} = \begin{bmatrix} 0^{3\times3} & I^{3\times3} & 0^{3\times7} \end{bmatrix},$$

$$\frac{\partial \dot{\boldsymbol{V}}}{\partial \bar{\boldsymbol{x}}} = \begin{bmatrix} \frac{\partial \dot{\boldsymbol{V}}}{\partial \boldsymbol{r}} & 0^{3\times3} & \frac{\partial \dot{\boldsymbol{V}}}{\partial m} & 0^{3\times3} & \frac{\partial \dot{\boldsymbol{V}}}{\partial \boldsymbol{p}_V} \end{bmatrix},$$

$$\frac{\partial \dot{m}}{\partial \bar{\boldsymbol{x}}} = \begin{bmatrix} 0^{1\times7} \end{bmatrix}$$

$$\frac{\partial \dot{\boldsymbol{p}}_r}{\partial \bar{\boldsymbol{x}}} = \begin{bmatrix} \frac{\partial \dot{\boldsymbol{p}}_r}{\partial \boldsymbol{r}} & 0^{3\times7} & \frac{\partial \dot{\boldsymbol{p}}_r}{\partial \boldsymbol{p}_V} \end{bmatrix},$$

$$\frac{\partial \boldsymbol{p}_V}{\partial \bar{\boldsymbol{x}}} = \begin{bmatrix} 0^{3\times7} & I^{3\times3} & 0^{3\times3} \end{bmatrix}$$

where

$$\frac{\partial \dot{\boldsymbol{V}}}{\partial \boldsymbol{r}} = \begin{bmatrix} -\frac{1}{\|\boldsymbol{r}\|^3} + \frac{3r_x^2}{\|\boldsymbol{r}\|^5} & \frac{3r_x r_y}{\|\boldsymbol{r}\|^5} & \frac{3r_x r_z}{\|\boldsymbol{r}\|^5} \\ \frac{3r_x r_y}{\|\boldsymbol{r}\|^5} & -\frac{1}{\|\boldsymbol{r}\|^3} + \frac{3r_y^2}{\|\boldsymbol{r}\|^5} & \frac{3r_y r_z}{\|\boldsymbol{r}\|^5} \\ \frac{3r_x r_z}{\|\boldsymbol{r}\|^5} & \frac{3r_y r_z}{\|\boldsymbol{r}\|^5} & -\frac{1}{\|\boldsymbol{r}\|^3} + \frac{3r_z^2}{\|\boldsymbol{r}\|^5} \end{bmatrix},$$

$$\frac{\partial \dot{\boldsymbol{V}}}{\partial m} = \begin{bmatrix} -\frac{Tp_{Vx}}{m^2 g_0 \|\boldsymbol{p}_V\|} \\ -\frac{Tp_{Vy}}{m^2 g_0 \|\boldsymbol{p}_V\|} \\ -\frac{Tp_{Vz}}{m^2 g_0 \|\boldsymbol{p}_V\|} \end{bmatrix}$$

$$\frac{\partial \dot{\boldsymbol{V}}}{\partial \boldsymbol{p}_V} = \frac{T}{mg_0} \begin{bmatrix} \frac{1}{\|\boldsymbol{p}_V\|} - \frac{p_{Vx}^2}{\|\boldsymbol{p}_V\|^3} & -\frac{p_{Vx}p_{Vy}}{\|\boldsymbol{p}_V\|^3} & -\frac{p_{Vx}p_{Vz}}{\|\boldsymbol{p}_V\|^3} \\ -\frac{p_{Vx}p_{Vy}}{\|\boldsymbol{p}_V\|^3} & \frac{1}{\|\boldsymbol{p}_V\|} - \frac{p_{Vy}^2}{\|\boldsymbol{p}_V\|^3} & -\frac{p_{Vy}p_{Vz}}{\|\boldsymbol{p}_V\|^3} \\ -\frac{p_{Vx}p_{Vz}}{\|\boldsymbol{p}_V\|^3} & -\frac{p_{Vy}p_{Vz}}{\|\boldsymbol{p}_V\|^3} & \frac{1}{\|\boldsymbol{p}_V\|} - \frac{p_{Vz}^2}{\|\boldsymbol{p}_V\|^3} \end{bmatrix}$$

$$\frac{\partial \dot{\boldsymbol{p}}_r}{\partial \boldsymbol{r}} = \begin{bmatrix} -\frac{3p_{Vx}r_x}{\|\boldsymbol{r}\|^5} - \frac{3\left(\boldsymbol{p}_V^T\boldsymbol{r} + p_{Vx}r_x\right)}{\|\boldsymbol{r}\|^5} + \frac{15\boldsymbol{p}_V^T\boldsymbol{r}r_x^2}{\|\boldsymbol{r}\|^7} & -\frac{3p_{Vx}r_y}{\|\boldsymbol{r}\|^5} - \frac{3p_{Vy}r_x}{\|\boldsymbol{r}\|^5} + \frac{15\boldsymbol{p}_V^T\boldsymbol{r}r_x r_y}{\|\boldsymbol{r}\|^7} & -\frac{3p_{Vx}r_z}{\|\boldsymbol{r}\|^5} - \frac{3p_{Vz}r_x}{\|\boldsymbol{r}\|^5} + \frac{15\boldsymbol{p}_V^T\boldsymbol{r}r_x r_z}{\|\boldsymbol{r}\|^7} \\ -\frac{3p_{Vy}r_x}{\|\boldsymbol{r}\|^5} - \frac{3p_{Vx}r_y}{\|\boldsymbol{r}\|^5} + \frac{15\boldsymbol{p}_V^T\boldsymbol{r}r_x r_y}{\|\boldsymbol{r}\|^7} & -\frac{3p_{Vy}r_y}{\|\boldsymbol{r}\|^5} - \frac{3\left(\boldsymbol{p}_V^T\boldsymbol{r} + p_{Vy}r_y\right)}{\|\boldsymbol{r}\|^5} + \frac{15\boldsymbol{p}_V^T\boldsymbol{r}r_y^2}{\|\boldsymbol{r}\|^7} & -\frac{3p_{Vy}r_z}{\|\boldsymbol{r}\|^5} - \frac{3p_{Vz}r_y}{\|\boldsymbol{r}\|^5} + \frac{15\boldsymbol{p}_V^T\boldsymbol{r}r_y r_z}{\|\boldsymbol{r}\|^7} \\ -\frac{3p_{Vz}r_x}{\|\boldsymbol{r}\|^5} - \frac{3p_{Vx}r_z}{\|\boldsymbol{r}\|^5} + \frac{15\boldsymbol{p}_V^T\boldsymbol{r}r_x r_z}{\|\boldsymbol{r}\|^7} & -\frac{3p_{Vz}r_y}{\|\boldsymbol{r}\|^5} - \frac{3p_{Vy}r_z}{\|\boldsymbol{r}\|^5} + \frac{15\boldsymbol{p}_V^T\boldsymbol{r}r_y r_z}{\|\boldsymbol{r}\|^7} & -\frac{3p_{Vz}r_z}{\|\boldsymbol{r}\|^5} - \frac{3\left(\boldsymbol{p}_V^T\boldsymbol{r} + p_{Vz}r\right)}{\|\boldsymbol{r}\|^5} + \frac{15\boldsymbol{p}_V^T\boldsymbol{r}r_z^2}{\|\boldsymbol{r}\|^7} \end{bmatrix}$$

$$\frac{\partial \dot{\boldsymbol{p}}_r}{\partial \boldsymbol{p}_V} = \begin{bmatrix} -\frac{1}{\|\boldsymbol{r}\|^3} - \frac{3r_x^2}{\|\boldsymbol{r}\|^5} & -\frac{3r_x r_y}{\|\boldsymbol{r}\|^5} & -\frac{3r_x r_z}{\|\boldsymbol{r}\|^5} \\ -\frac{3r_x r_y}{\|\boldsymbol{r}\|^5} & -\frac{1}{\|\boldsymbol{r}\|^3} - \frac{3r_y^2}{\|\boldsymbol{r}\|^5} & -\frac{3r_y r_z}{\|\boldsymbol{r}\|^5} \\ -\frac{3r_x r_z}{\|\boldsymbol{r}\|^5} & -\frac{3r_y r_z}{\|\boldsymbol{r}\|^5} & -\frac{1}{\|\boldsymbol{r}\|^3} - \frac{3r_z^2}{\|\boldsymbol{r}\|^5} \end{bmatrix}$$

REFERENCES

[1] P. Lu and X. Liu, "Autonomous trajectory planning for rendezvous and proximity operations by conic optimization," *J. Guid., Control, Dyn.*, vol. 36, no. 2, pp. 375–389, 2013.

[2] Y. Ling, Y. Zhou, and Q. Luo, "Lévy flight trajectory-based whale optimization algorithm for global optimization," *IEEE Access*, vol. 5, pp. 6168–6186, 2017.

[3] C. Parzani and S. Puechmorel, "On a Hamilton-Jacobi-Bellman approach for coordinated optimal aircraft trajectories planning," *Optim. Control Appl. Methods*, vol. 39, no. 2, pp. 933–948, 2018.

[4] O. Cots, J. Gergaud, and D. Goubinat, "Direct and indirect methods in optimal control with state constraints and the climbing trajectory of an aircraft," *Optim. Control Appl. Methods*, vol. 39, no. 1, pp. 281–301, 2018.

[5] R. Chai, A. Tsourdos, A. Savvaris, S. Chai, and Y. Xia, "Two-stage trajectory optimization for autonomous ground vehicles parking maneuver," *IEEE Trans. Ind. Informat.*, vol. 15, no. 7, pp. 3899–3909, Jul. 2017.

[6] R. Chai, A. Savvaris, A. Tsourdos, Y. Xia, and S. Chai, "Solving multiobjective constrained trajectory optimization problem by an extended evolutionary algorithm," *IEEE Trans. Cybern.*, to be published.

[7] H.-X. Shen, "No-guess indirect optimization of asteroid mission using electric propulsion," *Optim. Control Appl. Methods*, vol. 39, no. 2, pp. 1061–1070, 2018.

[8] B. Pan, P. Lu, X. Pan, and Y. Ma, "Double-homotopy method for solving optimal control problems," *J. Guid., Control, Dyn.*, vol. 39, no. 8, pp. 1706–1720, 2016.

[9] B. Pan, Z. Chen, P. Lu, and B. Gao, "Reduced transversality conditions in optimal space trajectories," *J. Guid., Control, Dyn.*, vol. 36, no. 5, pp. 1289–1300, 2013.

[10] P. Lu and B. F. Pan, "Highly constrained optimal launch ascent guidance," *J. Guid., Control, Dyn.*, vol. 33, no. 2, pp. 404–414, Mar. 2010.

[11] M. H. Gräßlin, J. Telaar, and U. M. Schöttle, "Ascent and reentry guidance concept based on NLP-methods," *Acta Astronaut.*, vol. 55, nos. 3–9, pp. 461–471, 2004.

[12] R. Chai, A. Savvaris, A. Tsourdos, S. Chai, Y. Xia, "Stochastic spacecraft trajectory optimization with the consideration of chance constraints," *IEEE Trans. Control Syst. Technol.*, to be published.

[13] R. Chai, A. Savvaris, A. Tsourdos, S. Chai, and Y. Xia, "Trajectory optimization of space maneuver vehicle using a hybrid optimal control solver," *IEEE Trans. Cybern.*, vol. 49, no. 2, pp. 467–480, Feb. 2019.

[14] X. Liu, "Autonomous trajectory planning by convex optimization," Ph.D. dissertation, Iowa State Univ., Ames, IA, USA, 2013.

[15] X. Liu, P. Lu, and B. Pan, "Survey of convex optimization for aerospace applications," *Astrodynamics*, vol. 1, no. 1, pp. 23–40, Sep. 2017.

[16] B. Açikmeşe and L. Blackmore, "Lossless convexification of a class of optimal control problems with non-convex control constraints," *Automatica*, vol. 47, no. 2, pp. 341–347, Feb. 2011.

[17] L. Blackmore, B. Açikmese, and J. M. Carson, III, "Lossless convexification of control constraints for a class of nonlinear optimal control problems," *Syst. Control Lett.*, vol. 61, no. 8, pp. 863–870, 2012.

[18] M. W. Harris and B. Açikmese, "Lossless convexification of non-convex optimal control problems for state constrained linear systems," *Automatica*, vol. 50, no. 9, pp. 2304–2311, 2014.

[19] Z. Zhang, J. Wang, and J. Li, "Lossless convexification of nonconvex MINLP on the UAV path-planning problem," *Optim. Control Appl. Methods*, vol. 39, no. 2, pp. 845–859, 2018.

[20] B. Acikmese and S. R. Ploen, "Convex programming approach to powered descent guidance for mars landing," *J. Guid., Control, Dyn.*, vol. 30, no. 5, pp. 1353–1366, 2007.

[21] X. Cheng, H. Li, and R. Zhang, "Efficient ascent trajectory optimization using convex models based on the Newton–Kantorovich/Pseudospectral approach," *Aerosp. Sci. Technol.*, vol. 66, pp. 140–151, Jul. 2017.

[22] K. Zhang, S. Yang, and F. Xiong, "Rapid ascent trajectory optimization for guided rockets via sequential convex programming," *Proc. Inst. Mech. Eng. G, J. Aerosp. Eng.*, vol. 233, no. 13, pp. 4800–4809, 2019.

[23] Z. Zhang, J. Li, and J. Wang, "Sequential convex programming for nonlinear optimal control problems in UAV path planning," *Aerosp. Sci. Technol.*, vol. 76, pp. 280–290, May 2018.

[24] D. Zhou, Y. Zhang, and S. Li, "Receding horizon guidance and control using sequential convex programming for spacecraft 6-DOF close proximity," *Aerosp. Sci. Technol.*, vol. 87, pp. 459–477, Apr. 2019.

[25] Z. Wang, "Optimal trajectories and normal load analysis of hypersonic glide vehicles via convex optimization," *Aerosp. Sci. Technol.*, vol. 87, pp. 357–368, Apr. 2019.

[26] Y. Zhang, W. Wang, Y. Zhang, and W. Sun, "Convex optimization for array diagnosis using amplitude-only far field data in impulsive noise environment," *IEEE Access*, vol. 7, pp. 14035–14043, 2019.

[27] T. Yokota and H. Hontani, "Simultaneous tensor completion and denoising by noise inequality constrained convex optimization," *IEEE Access*, vol. 7, pp. 15669–15682, 2019.

[28] H. Sun, "Closed-loop endo-atmospheric ascent guidance for reusable launch vehicle," Ph.D. dissertation, Dept. Aerosp. Eng., Iowa State Univ., Ames, IA, USA, 2005.

[29] H. D. Curtis, *Orbital Mechanics for Engineering Students*. Oxford, U.K.: Butterworth-Heinemann, 2013.

[30] M. Sagliano, "Pseudospectral convex optimization for powered descent and landing," *J. Guid., Control, Dyn.*, vol. 41, no. 2, pp. 320–334, 2017.

[31] D. Garg, "Advances in global pseudospectral methods for optimal control," Ph.D. dissertation, Univ. Florida, Gainesville, FL, USA, 2011.

[32] J. Wang, N. Cui, and C. Wei, "Optimal rocket landing guidance using convex optimization and model predictive control," *J. Guid., Control, Dyn.*, vol. 42, no. 5, pp. 1078–1092, 2019.

[33] M. Grant and S. Boyd. (2016). *CVX: MATLAB Software for Disciplined Convex Programming, Version 2.1*. [Online]. Available: http://cvxr.com/cvx/

[34] M. A. Patterson and V. A. Rao, "GPOPS-II: A MATLAB software for solving multiple-phase optimal control problems using HP-adaptive Gaussian quadrature collocation methods and sparse nonlinear programming," *ACM Trans. Math. Softw.*, vol. 41, no. 1, 2014, Art. no. 1.

YUAN LI received the B.S. degree in flight vehicle design and engineering from the Harbin Institute of Technology, Harbin, China, in 2015, where he is currently pursuing the Ph.D. degree in aeronautical and astronautical science and technology. His research interests include advanced guidance and control methods of flight vehicle, convex optimization theory and application, and robust control and application.

YINGZI GUAN received the M.E. degree in rocket engine from the Nanjing University of Science and Technology, in 1993, and the D.E. degree in aircraft design from the Harbin Institute of Technology (HIT), in 2000. She has been a Professor with the Department of Aerospace Engineering, HIT, in 2005, and a Committee Member of the Space Optics and Electromechanics Committee of Space Science Academy. Her main research directions include dynamics and control of spacecraft, simulation, and design of space agencies dynamics, development of aircraft ground simulation equipment. She received the Third Prize of the National Defense Science and Technology Progress Award four times and has issued over 20 professional theses.

CHANGZHU WEI received the B.S. degree in flight vehicle design and engineering from the Harbin Institute of Technology, Harbin, China, in 2005, and the Ph.D. degree in aeronautical and astronautical science and technology from the Harbin Institute of Technology, Harbin, in 2010. From 2013 to 2015, he was an Assistant Professor with the School of Astronautics, Harbin Institute of Technology, Harbin, where he has been an Associate Professor with the School of Astronautics, since 2016. He is the author of one book, more than 30 articles, and two inventions. His research interests include advanced guidance and control methods of flight vehicle, and trajectory design and optimization of flight vehicle.

RENYI HU received the B.S. degree in measurement and control technology and instrumentation program from Harbin Engineering University, Harbin, China, in 2006, and the master's degree from China Academy, Beijing, China, in 2009. Since 2009, he has been with the Beijing Aerospace Automatic Control Institute. His main research interests include dynamics and control of spacecraft, simulation, advanced guidance, and control methods.